Preprints (www.preprints.org) | NOT PEER-REVIEWED | Posted: 28 December 2018 doi:10.20944/preprints201812.0347.v1

Peer-reviewed version available at *Sensors* **2019**, *19*, 641; doi:10.3390/s19030641

Article

Haptic glove and platform with gestural control for neuromorphic tactile sensory feedback in medical telepresence†

Jessica D'Abbraccio[1,*], Luca Massari[1,*], Sahana Prasanna[1], Laura Baldini[2], Francesca Sorgini[1], Giuseppe Airò Farulla[3], Andrea Bulletti[4], Marina Mazzoni[4,5], Lorenzo Capineri[4], Arianna Menciassi[1], Petar Petrovic[6,7], Eduardo Palermo[2], Calogero Maria Oddo[1,]**

[1] Sant'Anna School of Advanced Studies, The BioRobotics Institute, 56025 Pisa, Italy; jessica.dabbraccio@santannapisa.it (J.D.A.); luca.massari@santannapisa.it (L.M.); sahana.prasanna@santannapisa.it (S.P.); francesca.sorgini@santannapisa.it (F.S.); arianna.menciassi@santannapisa.it (A.M.)

[2] Department of Mechanical and Aerospace Engineering, "Sapienza" University of Rome, 00185 Rome, Italy; laurabaldini93@gmail.com (L.B.); eduardo.palermo@uniroma1.it (E.P.)

[3] Department of Control and Computer Engineering, Politecnico di Torino, 10129 Turin, Italy; giuseppe.airof@gmail.com (G.A.F.)

[4] Department of Information Engineering, Università degli studi di Firenze, 50121 Florence, Italy; andrea.bulletti@unifi.it (A.B.); lorenzo.capineri@unifi.it (L.C.)

[5] Consiglio Nazionale delle Ricerche of Italy, Istituto di Fisica Applicata "Nello Carrara", Florence, Italy; m.mazzoni@ifac.cnr.it (M.M.)

[6] Production Engineering Department, Faculty of Mechanical Engineering, University of Belgrade, 11120 Belgrade, Serbia; pbpetrovic@mas.bg.ac.rs (P.B.P.)

[7] Academy of Engineering Sciences of Serbia (AISS), Belgrade, Serbia

† This paper is an extended version of our paper published in the 2018 IEEE International Symposium on Medical Measurements and Applications (MeMeA)

*These authors share first authorship based on equal contribution

**Correspondence: calogero.oddo@santannapisa.it (C.M.O.); +39-050-883067

Abstract: The advancements in the study of the human sense of touch are fueling the field of haptics. This is paving the way for augmenting the sensory perception during objects palpation in tele-surgery, and reproducing the information through tactile feedback. Here, we present a novel tele-palpation apparatus that enables the user to detect nodules with various distinct stiffness buried in an *ad-hoc* polymeric phantom. The contact force measured by the platform was encoded using a neuromorphic model and reproduced on the index fingertip of a remote user through a haptic glove embedding a piezoelectric disk. We assessed the effectiveness of this feedback in allowing nodule identification under two experimental conditions of real-time telepresence: In Line of Sight (ILS), where the platform was placed in the visible range of a user; and the more demanding Not In Line of Sight (NILS), with the platform being 50 km apart. We found that the entailed percentage of identification was higher for stiffer inclusions with respect to the softer ones (average of 74% within the duration of the task), in both telepresence conditions evaluated. These promising results call for further exploration of tactile augmentation technology for telepresence in medical interventions.

Keywords: Nodules detection, neuromorphic touch, polymeric phantom, sensory augmentation, tactile telepresence, teleoperation, tele-palpation, vibro-tactile stimulation.

© 2018 by the author(s). Distributed under a Creative Commons CC BY license.

Preprints (www.preprints.org) | NOT PEER-REVIEWED | Posted: 28 December 2018 doi:10.20944/preprints201812.0347.v1

Peer-reviewed version available at Sensors 2019, 19, 641; doi:10.3390/s19030641

1. Introduction

The impact of haptic devices has tremendously grown over the last decade [1,2]. Contributions from diverse research fields are fueling the study of human sense of touch, such as measurement and instrumentation, biomedical engineering, cognitive science and neuroscience, robotics and biorobotics, computer graphics and psychophysics. In this vein, studies focused on the development of haptic devices or artificial tactile sensors are becoming prominent. In particular, literature is populated with solutions in the field of telerobotics, which refers to a broad range of different applications, from virtual reality simulations and sensory substitution to teleoperations and telepresence [3-14].

Beyond these applications, tactile technologies employed in telepresence and teleoperation scenarios have been widely used in the field of minimally invasive surgery (MIS) and robotic minimally invasive surgery (RMIS), to overcome the absence of both tactile and force feedback conveyed to the physician. Feedback is crucial for helping the surgeon to preserve healthy tissues, as well as for detecting differences in stiffness throughout the palpated sites [15–20]. Despite the growth in recent interest and research, the degree of maturity of touch sensing is still lagging behind that of other perceptive technologies, such as audio or computer vision [21–26].

A plausible explanation is in the biological complexity of the sense of touch, where the distributed sensitized region covers the entire body [27], while other human senses have localized sensitive areas. Research in tactile field focuses mainly on the human hand, in particular fingertips, being regions with densely populated and functionally diverse skin receptors [28,29]. This spatial density allows for a high resolution, and encodes a wide range of temporal and spatial stimulation [30–33]. Although passive touch conveys information about the miscellaneous properties of the explored object, an *active exploration* permits enrichment of the tactile signals, thanks to integration with the proprioceptive input from the joints.

In a previous work [34], we developed a mechatronic platform interfaced with a vibro-tactile glove for tactile augmentation in telepresence. The results demonstrated the efficiency of the system in presenting mechanical information about test objects. The stiffness of different materials, converted into spikes with proper frequency through a neural model, was used to drive piezoelectric disks embedded in the index and the thumb of a vibro-tactile glove. The designed psychophysical protocol for discriminating stiffness, tested with 2-Alternative Forced Choice passive touch, unveiled specific perceptual thresholds, derived using Ulrich-Miller Cumulative Distribution Function.

Building on the findings of the previous study, here we propose a telepresence system with active exploration of a silicon phantom that embeds elements with different stiffness within. In this condition, the user can directly control and move the indenting platform, with an additional optical sensor for tracking the hand movements. We investigated two experimental conditions of telepresence: i) ILS, where the platform was placed In Line of Sight of the user [35], ii) NILS, where the platform was Not In Line of Sight, in a different location with respect to the user, for a more challenging task. Hence, the objective of the present study is to investigate the mechanisms of tactile perception under active gestural control and the effectiveness of the proposed spike-based feedback strategy. In particular, the delivered vibro-tactile feedback mimics the language of tactile receptors, generated by a neuromorphic model [36–38].

2. Materials and Methods

2.1. Experimental setup

The experimental apparatus was composed by two essential sub-setups, positioned at a proper distance for achieving telepresence condition (Figure *1*).

Preprints (www.preprints.org) | NOT PEER-REVIEWED | Posted: 28 December 2018 doi:10.20944/preprints201812.0347.v1

Peer-reviewed version available at Sensors 2019, 19, 641; doi:10.3390/s19030641

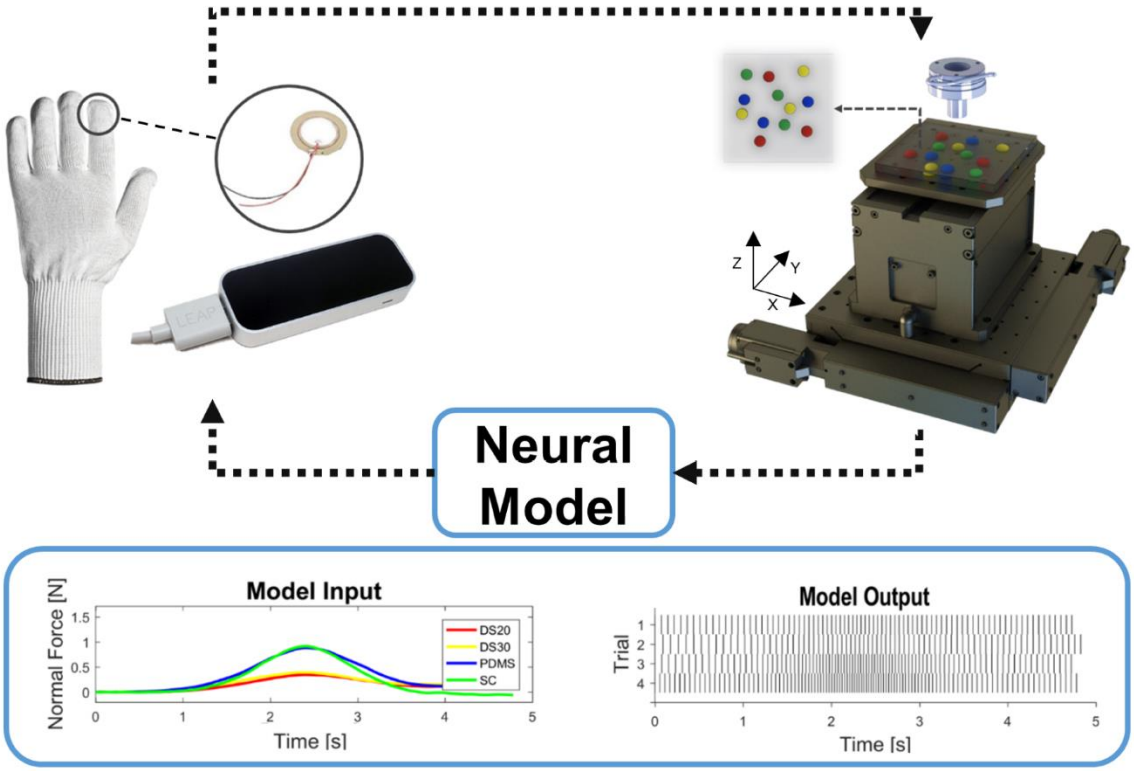

Figure 1. Experimental apparatus. Left: the haptic sub-system comprising a textile glove with a detail of the encapsulated piezoelectric disk for index fingertip vibro-tactile stimulation and optical sensor for hand gesture tracking; right: tactile sub-system comprising a 3-axis cartesian manipulator with load cell and the indenter, and a detail on the silicon phantom displaying nodules placement. The two sub-setups were spatially separated to achieve ILS and NILS telepresence conditions. The plots at the bottom of the figure show the neural encoding of the normal force arising during the sliding phase of the phantom into spike trains for all the polymers, from the softest (red) to the hardest (green).

The first sub-setup consisted of a piezoelectric disk (7BB-12-9, MuRata, Kyoto Prefecture, Japan) encapsulated in a silicone rubber, with a customized process, that was placed at index fingertip of a textile glove to deliver the feedback [39]. An optical sensor (Leap Motion, CA, USA) tracked the user's hand gesture. We defined as *haptic sub-system* this first sub-setup located in a laboratory of The BioRobotics Institute of Sant'Anna School of Advanced Studies, Pontedera (Pisa, Italy). A graphical user interface (GUI) was developed using LabVIEW (National Instruments Corp., USA) for acquiring speed and position of the hand's center of mass, handling communication with the other remote sub-setup and recording hand position data.

We defined as *tactile sub-system*, the second remote sub-setup used for the exploration of the phantom. This platform included: a cartesian manipulator (X-Y and Z, 8MTF-102LS05 and 8MVT120-25- 4247, STANDA, Vilnius, Lithuania); a 6-axis load cell (Nano 43, ATI Industrial Automation, Apex, USA) to measure contact forces between a customized indenter with a spherical tip of 3 mm radius, mounted on the load cell, and the phantom during the active sliding. A second GUI was designed for real-time control of the motorized stages and data communication.

In the ILS session, the *tactile sub-system* was placed near the user, to perform experiments in streamlined telepresence. In the NILS session, instead, it was located in a remote laboratory in Florence, Italy, that was about 50 km apart from the *haptic sub-system*, thus to increase the challenge of the proposed task. Data communication between the two sub-setups was provided through the User Datagram Protocol (UDP) that ensured a maximum latency of 15 ms. The adopted communication protocol allowed bidirectional streaming of data: hand gesture from the haptic sub-

Preprints (www.preprints.org) | NOT PEER-REVIEWED | Posted: 28 December 2018 doi:10.20944/preprints201812.0347.v1

Peer-reviewed version available at Sensors 2019, 19, 641; doi:10.3390/s19030641

system to the mechatronic platform, normal force from the tactile sub-system to the glove to be encoded and then delivered (Figure 2).

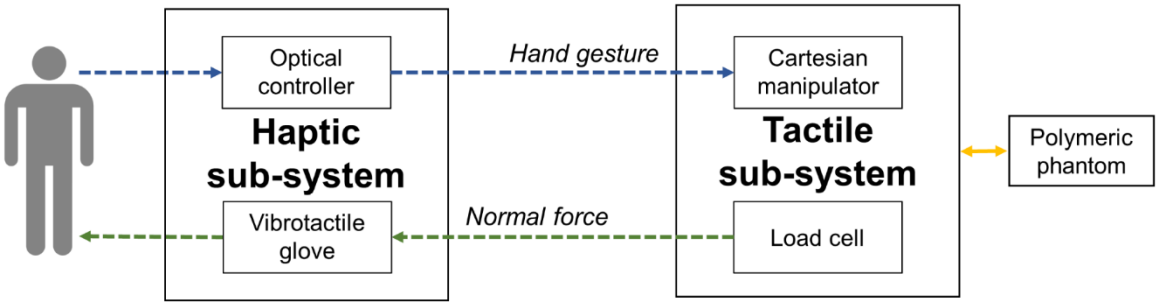

Figure 2. Block diagram: bidirectional data streaming between the haptic and tactile sub-systems provided via UDP: the optical controller conveyed speed and position of the center of mass of user's hand from the first environment to the cartesian manipulator in the remote one (blue arrow) and, while sliding, normal force data collected by the load cell from the platform to the vibro-tactile glove to deliver the spike-based stimulation (green arrow).

During experiments, the user actively explored and searched for stiffer areas in the polymeric phantom. Four different rubber materials were used to cast 12 hemispherical inclusions (3 replicas of each material), of 5 mm radius, randomly inserted across the X-Y plane in a silicon cuboidal block, 100 x 100 x 15 mm^3 in size. The chosen polymers for the inclusions were: Sorta Clear 40 (Smooth-on, PA, USA), as the stiffest, Polydimethylsiloxane (PDMS) Sylgard 184 (Dow Corning, USA), Dragon Skin 30 and Dragon Skin 20, while Dragon Skin 10, the softest, was used for the cuboidal block. Before involving human subjects, the phantom was mechanically characterized to assess the vertical stiffness ($\Delta F_z/\Delta z$) of the nodules and the surrounding soft material by means of the proposed platform equipped with a flat indenter. The adopted experimental protocol consisted of 5 trials in which the entire set of inclusions experienced an indentation at a fixed force threshold (F_z = 0.5 N) and speed (v= 0.125 mms^{-1}). To estimate the stiffness of the investigated polymers, the vertical component of the force collected during each compression was processed through scripts in Matlab (R2016b, MathWorks, MA, USA) and results of such a characterization were reported in Section 3.

The platform control during the experimental session was based on the user's hand movements, tracked by the 3-D optical sensor. To provide user with resting volume in the reference system of the optical controller, a virtual sphere was initially set at the origin. As user's hand moved out of this volume, the motorized stages followed along the same direction at a speed proportional to the displacement of the user's hand. The assigned speed was calculated using the difference $\varrho - \varrho_0$, where ϱ was the distance between the hand center of mass and the center of the sensor, and ϱ_0 was the radius of the neutral spherical region, set to 50 mm. The user was provided with a visual feedback about the position of the indenter on the phantom in the remote environment, without any information on the location of the inclusions. The contact between the indenter tip and the polymeric test object generated a force. To avoid mechanical damage to phantom and load cell due to users' upward movement, a force threshold (0.5 N) was introduced. The measured force was sent to the haptic sub-system to be encoded into spike patterns, that triggered the piezoelectric actuator. We implemented a neuromorphic feedback strategy based on a regular Izhikevich spiking model (F_{th}=0.08 N; A=0.04 $mS^{-1}mV^{-1}$; B=5 ms^{-1}; C=140 $mVms^{-1}$; a=0.02 ms^{-1} b=0.2 ms^{-1}; c=-65 mV; d=8 mV; V_{th}=30 mV; k=10 $mVms^{-1}N^{-1}$; dt =0.2ms), discretized using Euler's method at 5 kHz [40]. The chosen model efficiently encodes the temporal dynamics of a mechanoreceptor including the biological plausibility of computationally intense Hodgkin-Huxley model [41] and the computational efficiency of integrate-and-fire model [42]. Through the model we tracked two variables v and u (see Eq. (1)-(4)), representing the membrane potential and the membrane recovery, respectively. The model is governed by the following equations:

Preprints (www.preprints.org) | NOT PEER-REVIEWED | Posted: 28 December 2018 doi:10.20944/preprints201812.0347.v1

Peer-reviewed version available at Sensors 2019, 19, 641; doi:10.3390/s19030641

$$If\ (F_z - F_{th}) > 0, then\ F_{in} = (F_z - F_{th}), \text{else}\ F_{in} = 0 \quad (1)$$

$$v_{n+1} = v_n + (Av_n^2 + Bv_n + C - u_n + kF_{in})dt \quad (2)$$

$$u_{n+1} = u_n + a(bv_n - u_n)dt \quad (3)$$

With the membrane potential reset condition:

$$\text{if } v_{n+1} \geq V_{th}, \text{then } \begin{cases} v_{n+1} \leftarrow c \\ u_{n+1} \leftarrow u_n + d \end{cases} \quad (4)$$

The neuromorphic activation of the transducer was achieved by setting the input to the neuron proportional to the magnitude of the normal force measured by the remote subsystem. Initial calibrations were also performed to counterbalance the effect of saturation of the neural model [35].

The spikes generated by the Izhikevich model were sent to the vibro-tactile glove by means of a piezoelectric driver (DRV2667, Texas Instruments). This driver facilitated in setting the actuation parameters in analog mode to have a gain of 40.7 dB, 200 V peak-to-peak voltage amplitude, and 105 V offset voltage.

2.2. Psychophysical Experiments

Psychophysical experiments were performed to validate the proposed system for delivering stiffness information about the palpated nodules in both ILS and NILS tactile telepresence conditions. The experiments involved 10 participants (7 men and 3 women between 24 and 33 years of age) in ILS, and 15 (9 men and 6 women between 25 and 37 years of age) in NILS, enrolled among the university students or staff of The BioRobotics Institute of Sant'Anna School of Advanced Studies, Pisa, Italy. The participants took a comfortable posture at the control workstation in the laboratory, where the haptic sub-system was located. They wore the vibro-tactile glove on their dominant hand and a headset to get rid of environmental noise. To familiarize with driving the tactile platform, each participant took part in a fifteen minutes training session. Moreover, this preliminary task got the users accustomed to the vibro-tactile signal exerted by the piezoelectric actuator of the glove. Answers provided during the training sessions were not included in the analyzed results. Both ILS and NILS psychophysical experiments consisted in a tactile identification task: within six minutes time-period of the protocol, the participants unreservedly explored the silicon block and pressed a button on a keyboard on any occasion of perceived frequency variation in the vibro-tactile feedback.

Performance of the participants were evaluated in Matlab (R2016b, MathWorks, MA, USA) in terms of rate of correct identification of the inclusions, using parameters calculated for both ILS and NILS populations and for each participant. Specifically, we evaluated: (a) the number of true positives, TP, (b) the number of false positives (FP) and (c) accuracy (TP/P, with P = collected responses - FP). These parameters were computed as a function of the center-to-center distance between the position of the perceived inclusions and the nearest actual inclusion. If the perceived position felt within a radius of 10 mm from the center of the nearest inclusion (i.e., the distance was equal to the diameter of the inclusion), the perceived inclusion was classified as TP, otherwise as FP. The classification of collected responses was also evaluated for a lower tolerance, 5 mm, and two greater ones, 15 mm and 20 mm. A logistic fitting, using a Cumulative Distribution Function (CFD) [43] and the *nlinfit* function of Matlab, was performed for each material to evaluate the rate of correct perception.

3. Results

In the preliminary phantom characterization, the stiffness of each material was measured by assuming the polymers having a linear response in the range of applied forces (Figure 3). According to the operated characterization, the stiffer materials were Sorta Clear (3.69 Nmm^{-1}) and PDMS (3.68 Nmm^{-1}), while Dragon skin 30 (2.88 Nmm^{-1}), Dragon skin 20 (2.74Nmm^{-1}) and Dragon skin 10 (2.14 Nmm^{-1}) showed lower values.

Preprints (www.preprints.org) | NOT PEER-REVIEWED | Posted: 28 December 2018 doi:10.20944/preprints201812.0347.v1

Peer-reviewed version available at Sensors 2019, 19, 641; doi:10.3390/s19030641

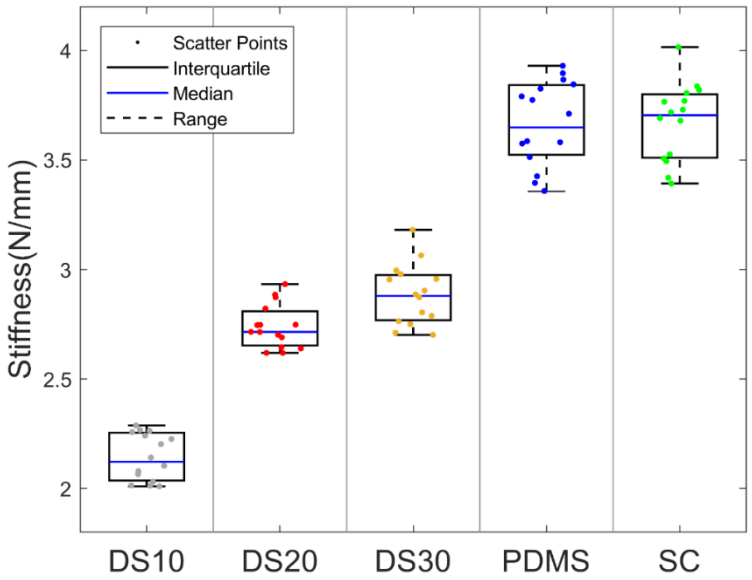

Figure 3. Mechanical characterization of the phantom: scatter points are the stiffness values collected for each material across the five trials of indentation; boxes represent interquartile ranges for the five materials; blue lines show the median values and black dashed lines the full ranges among the measured values.

In the psychophysical experiments with tactile feedback in ILS and NILS telepresence conditions, we successfully delivered a neuromorphic stimulation encoding the stiffness of the telepalpated phantom. The inclusions recognized by the user were recorded with key press. An example of the path followed and the responses is shown in Figure *4*.

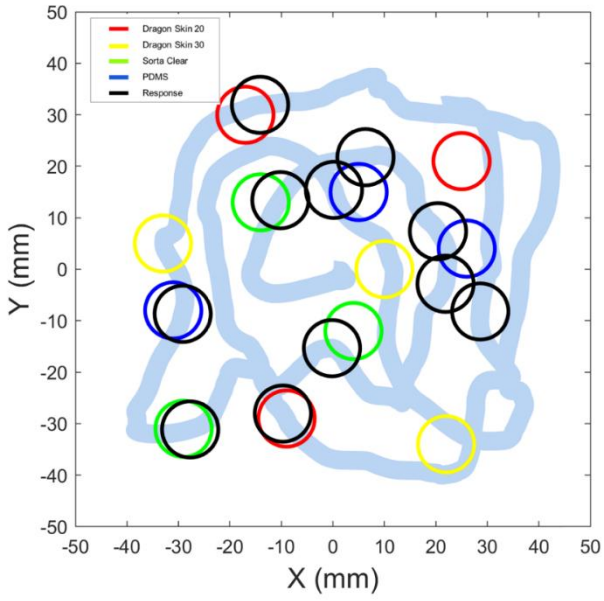

Figure 4. Example of responses given by a participant across an experimental session: colored circles mark the position of the inclusion set; black circles represent the position of the indenter when the subject pressed the key, and light blue line represents the trail of the probe on the phantom surface.

Results show that an average of 63% and 60% of the inclusions were correctly perceived and declared within a tolerance of 10 mm to the nearest inclusion, for ILS and NILS experiments, respectively. In both cases, with a tolerance higher than the inclusion diameter (i.e. >10 mm), the rate of identified inclusions was slightly higher (Figure *5*).

Preprints (www.preprints.org) | NOT PEER-REVIEWED | Posted: 28 December 2018 doi:10.20944/preprints201812.0347.v1

Peer-reviewed version available at Sensors 2019, 19, 641; doi:10.3390/s19030641

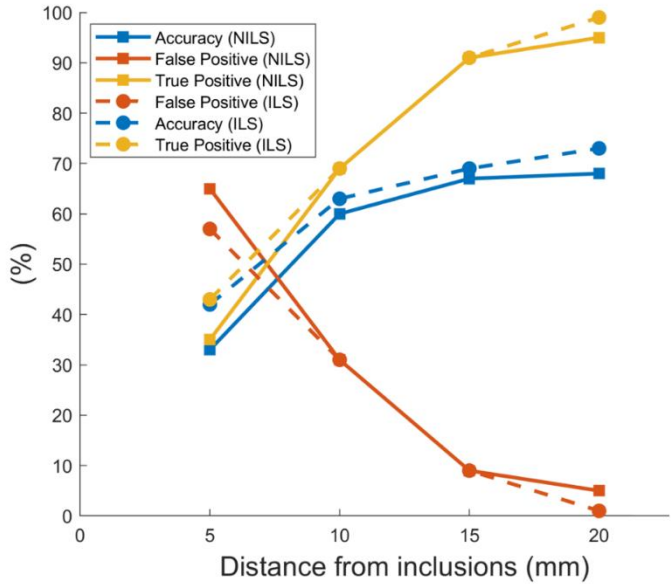

Figure 5. Tolerance of recognized inclusions: each point (dot for ILS and square for NILS) represents the mean accuracy (blue line), mean false positive (red line) and mean true positive (yellow line) responses evaluated through a classification based on the admitted center-to-center distance between perceived inclusions and the real ones.

The identification rate for all the participants, across populations, was evaluated for each material and is presented in Figure *6* with increasing stiffness along with the interquartile range (IQR) for the accuracy of declared inclusions. Performance, in terms of correct identification of inclusions, was 65% and 70% for stiffer stimuli including both the populations. The minimum accuracy in perceiving the inclusions with lower stiffness was found to be 52%, with the exception of the softest Dragon skin 20 material in NILS condition, whose rate decreased down to 33%. The global performance of identified inclusions, across all materials, showed an average of 63% and 60%, respectively for ILS and NILS conditions (Figure *6*).

$$G(x) = \left[1 + e^{-\frac{x-a}{b}}\right]^{-1} \tag{5}$$

The fitting function reported in Eq. (5), represents the probability of a correct response at a stiffness difference x, where a denotes the perceptual threshold, and $b > 0$ a scale parameter that affects the curve steepness. The final evaluation of the perception, found by fitting the response datasets into the CFD (eq. 5), demonstrates that the user could distinguish an inclusion with stiffness higher than $a = 2.5$ Nmm^{-1} and $a = 2.9$ Nmm^{-1} in ILS and NILS conditions, respectively (Figure *6*).

Preprints (www.preprints.org) | NOT PEER-REVIEWED | Posted: 28 December 2018 doi:10.20944/preprints201812.0347.v1

Peer-reviewed version available at Sensors 2019, 19, 641; doi:10.3390/s19030641

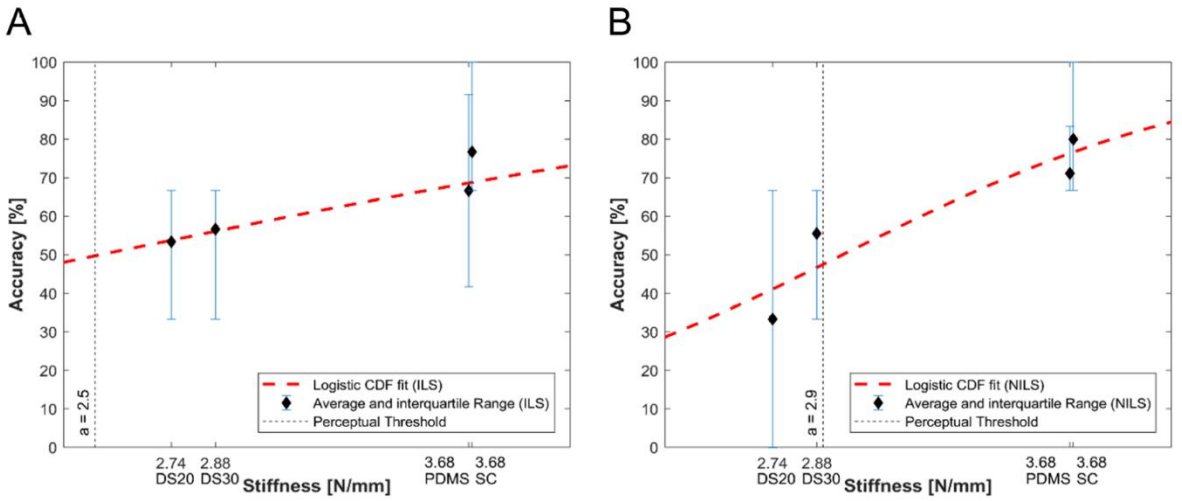

Figure 6. Psychometric curves for the psychophysical experiments: (A) ILS telepresence condition; (B) NILS telepresence condition. Black diamonds show the identification rate for all the encapsulated materials (average across participants); error bars are the interquartile range across participants; red dashed lines represent the logistic cumulative distribution function (CDF) fit.

4. Discussion and conclusion

This paper assesses the usability of the developed tactile system in tele-palpation to localize various stiffer polymeric nodules in the surrounding soft matrix during active exploration. The promising results demonstrate the ease and successful augmentation for the navigation in a soft terrain. The four types of inclusions are observed to be paired with respect to their stiffness values (Softer: DS20, DS30; Stiffer: PDMS, SC) that are also reflected in the user's accuracy graph.

The present study was conducted within two different telepresence conditions. Initially, in a more controlled environment, the sensing platform was placed near the user (in line of sight – ILS), while afterwards the platform was moved to a remote location (not in line of sight – NILS). This addressed two levels of challenge for the user: remote platform control and stiffness discrimination with the haptic glove. The intrinsic absence of vision of the platform in NILS with respect to ILS is phenomenally displayed in the perceptual thresholds (a = 2.9 and a = 2.5). Also, the network latency introduced a delay of the order of ms, demanding subject's attention to the active control, to coordinate the proprioceptive information with the moving platform, occasionally compromising attention from the sensory feedback. We showed that the presented tactile telepresence system enabled the correct discrimination of the inclusions throughout the polymeric matrix, especially for the stiffer ones, in both ILS and NILS telepresence conditions. This work enriches the findings of our previous works [34–37], confirming that the adoption of spike-like stimulation, emulating the firing activity of skin mechanoreceptors, offers a new language of feedback communication, to provide perceptual augmentation in tele-palpation with gestural active exploration.

Future works will be headed towards exploring the recognition amongst the stiffer materials in two aspects: upgrading the phantom for medical applications and enriching the mechanical information encoded. We will evaluate higher variations of materials stiffness towards the aim of discriminating healthy tissues from tumors, that are generally stiffer than the surroundings [44–46]. Furthermore, we will also include the evaluation of encoded feedback for both normal and shear components of the contact force through the neuromorphic model. This enrichment is expected to lead to a more detailed appreciation of stiffness in cases of anisotropic mechanical behavior of biomaterials.

Author Contributions:

J.D.A. co-designed the experimental protocol, integrated the experimental setup, performed the experimental protocol, analysed data, discussed the results and edited the paper; L.M. co-designed the experimental protocol, developed the mechatronic platform and integrated the experimental setup, performed the experimental

Preprints (www.preprints.org) | NOT PEER-REVIEWED | Posted: 28 December 2018 doi:10.20944/preprints201812.0347.v1

Peer-reviewed version available at Sensors 2019, 19, 641; doi:10.3390/s19030641

protocol, analysed data, discussed the results and edited the paper; S.P integrated the experimental setup, contributed to the experimental activities and to discussing the results, and edited the paper; L.B. co-designed the experimental protocol, integrated the experimental setup, contributed to the experimental activities and to data analysis, discussed the results and contributed to prepare the original draft of the paper; F.S developed the haptic glove and revised the paper; G.A.F. and P.B.P. contributed to developing the gesture based controller and revised the paper; A.B., M.M., L.C. and A.M contributed to the development of the mechatronic platform and revised the paper; E.P. co-designed and co-supervised experimental activities, contributed to discussing the results and to revising the paper; C.M.O designed and supervised the study, supervised the development of the whole experimental apparatus and contributed to its development, co-designed the experimental protocol, contributed to data analysis, discussed the results and wrote the paper.

Funding: This project received seed funding from the Dubai Future Foundation through Guaana.com open research platform and was in part funded by the Tuscany Region through the IMEROS project (D66D16000120002) activated within the PAR FAS 2007/2013 action 1.1.2, by the National Institute for Insurance against Accidents at Work (INAIL) through the MOTU project, by the Italian Ministry of Education, Universities and Research within the "Smart Cities and Social Innovation Under 30" program through the PARLOMA Project (SIN_00132), by the Italian Ministry of Foreign Affairs and International Cooperation via the Italy-Serbia bilateral project Human - Robot Co-Working as a Key Enabling Technology for the Factories of Future (project ID: PGR00758 / 2017).

Acknowledgments: The authors thank Dr. Alberto Mazzoni, Dr. Domenico Camboni and Mr. Riccardo Di Leonardo for their technical support.

Conflicts of Interest: The authors declare no conflict of interest. The funders had no role in the design of the study; in the collection, analyses, or interpretation for data; in the writing of the manuscript, or in the decision to publish the results.

References

1. Hannaford, B.; Okamura, A.M. Haptics. In *Springer Handbook of Robotics*; 2016 ISBN 978-3-540-30301-5.
2. Velázquez, R.; Pissaloux, E. Tactile Displays in Human-Machine Interaction : Four Case Studies. *Int. J. Virtual Real.* **2008**.
3. Varalakshmi, B.D.; Thriveni, J.; Venugopal, K.R.; Patnaik, L.M. Haptics: state of the art survey. *Int. J. Comput. Sci. Issues* **2012**, *9*, 234.
4. Bach-y-Rita, P.; Collins, C.C.; Saunders, F.A.; White, B.; Scadden, L. Vision substitution by tactile image projection. *Nature* **1969**, *221*, 963.
5. Sziebig, G.; Solvang, B.; Kiss, C.; Korondi, P. Vibro-tactile feedback for VR systems. In Proceedings of the Human System Interactions, 2009. HSI'09. 2nd Conference on; IEEE, 2009; pp. 406–410.
6. Yamamoto, T.; Abolhassani, N.; Jung, S.; Okamura, A.M.; Judkins, T.N. Augmented reality and haptic interfaces for robot-assisted surgery. *Int. J. Med. Robot. Comput. Assist. Surg.* **2012**, *8*, 45–56.
7. White, B.W. Perceptual findings with the vision-substitution system. *IEEE Trans. Man-Machine Syst.* **1970**, *11*, 54–58.
8. Collins, C.C. Tactile television-mechanical and electrical image projection. *IEEE Trans. man-machine Syst.* **1970**, *11*, 65–71.
9. Bliss, J.C.; Katcher, M.H.; Rogers, C.H.; Shepard, R.P. Optical-to-tactile image conversion for the blind. *IEEE Trans. Man-Machine Syst.* **1970**, *11*, 58–65.
10. Kaczmarek, K.A.; Webster, J.G.; Bach-y-Rita, P.; Tompkins, W.J. Electrotactile and vibrotactile displays for sensory substitution systems. *IEEE Trans. Biomed. Eng.* **1991**, *38*, 1–16.
11. Sparks, D.W.; Ardell, L.A.; Bourgeois, M.; Wiedmer, B.; Kuhl, P.K. Investigating the MESA (multipoint electrotactile speech aid): The transmission of connected discourse. *J. Acoust. Soc. Am.* **1979**, *65*, 810–815.
12. Sibert, J.; Cooper, J.; Covington, C.; Stefanovski, A.; Thompson, D.; Lindeman, R.W. Vibrotactile feedback for enhanced control of urban search and rescue robots. In Proceedings of the Proceedings of the IEEE International Workshop on Safety, Security and Rescue Robotics; 2006.

Preprints (www.preprints.org) | NOT PEER-REVIEWED | Posted: 28 December 2018 doi:10.20944/preprints201812.0347.v1

Peer-reviewed version available at Sensors 2019, 19, 641; doi:10.3390/s19030641

13. Choi, S.; Kuchenbecker, K.J. Vibrotactile display: Perception, technology, and applications. *Proc. IEEE* **2013**, *101*, 2093–2104.
14. Alahakone, A.U.; Senanayake, S.M.N.A. Vibrotactile feedback systems: Current trends in rehabilitation, sports and information display. In Proceedings of the Advanced Intelligent Mechatronics, 2009. AIM 2009. IEEE/ASME International Conference on; IEEE, 2009; pp. 1148–1153.
15. Pacchierotti, C.; Prattichizzo, D.; Kuchenbecker, K.J. Cutaneous feedback of fingertip deformation and vibration for palpation in robotic surgery. *IEEE Trans. Biomed. Eng.* **2016**, *63*, 278–287.
16. Van der Meijden, O.A.J.; Schijven, M.P. The value of haptic feedback in conventional and robot-assisted minimal invasive surgery and virtual reality training: a current review. *Surg. Endosc.* **2009**, *23*, 1180–1190.
17. Tavakoli, M.; Patel, R. V; Moallem, M. A force reflective master-slave system for minimally invasive surgery. In Proceedings of the Intelligent Robots and Systems, 2003.(IROS 2003). Proceedings. 2003 IEEE/RSJ International Conference on; IEEE, 2003; Vol. 4, pp. 3077–3082.
18. Peirs, J.; Clijnen, J.; Reynaerts, D.; Van Brussel, H.; Herijgers, P.; Corteville, B.; Boone, S. A micro optical force sensor for force feedback during minimally invasive robotic surgery. *Sensors Actuators A Phys.* **2004**, *115*, 447–455.
19. Tiwana, M.I.; Redmond, S.J.; Lovell, N.H. A review of tactile sensing technologies with applications in biomedical engineering. *Sensors Actuators A Phys.* **2012**, *179*, 17–31.
20. Hu, T.; Castellanos, A.E.; Tholey, G.; Desai, J.P. Real-time haptic feedback in laparoscopic tools for use in gastro-intestinal surgery. In Proceedings of the International Conference on Medical Image Computing and Computer-Assisted Intervention; Springer, 2002; pp. 66–74.
21. Lee, M.H.; Nicholls, H.R. Review Article Tactile sensing for mechatronics—a state of the art survey. *mechatronics* **1999**, *9*, 1–31.
22. Iwata, H.; Yano, H.; Uemura, T.; Moriya, T. Food simulator: A haptic interface for biting. In Proceedings of the Virtual Reality, 2004. Proceedings. IEEE; IEEE, 2004; pp. 51–57.
23. Ranasinghe, N.; Nakatsu, R.; Nii, H.; Gopalakrishnakone, P. Tongue mounted interface for digitally actuating the sense of taste. In Proceedings of the 2012 16th Annual International Symposium on Wearable Computers (ISWC); IEEE, 2012; pp. 80–87.
24. Ranasinghe, N.; Do, E.Y.-L. Digital lollipop: Studying electrical stimulation on the human tongue to simulate taste sensations. *ACM Trans. Multimed. Comput. Commun. Appl.* **2017**, *13*, 5.
25. Cruz, A.; Green, B.G. Thermal stimulation of taste. *Nature* **2000**, *403*, 889.
26. Wilson, A.D.; Baietto, M. Advances in electronic-nose technologies developed for biomedical applications. *Sensors* **2011**, *11*, 1105–1176.
27. Albini, A.; Denei, S.; Cannata, G. Human hand recognition from robotic skin measurements in human-robot physical interactions. In Proceedings of the IEEE International Conference on Intelligent Robots and Systems; 2017.
28. Caldwell, D.G.; Tsagarakis, N.; Wardle, A. Mechano thermo and proprioceptor feedback for integrated haptic feedback. In Proceedings of the Robotics and Automation, 1997. Proceedings., 1997 IEEE International Conference on; IEEE, 1997; Vol. 3, pp. 2491–2496.
29. Dahiya, R.S.; Metta, G.; Valle, M.; Sandini, G. Tactile sensing—from humans to humanoids. *IEEE Trans. Robot.* **2010**, *26*, 1–20.
30. Verrillo, R.T. Psychophysics of vibrotactile stimulation. *J. Acoust. Soc. Am.* **1985**, *77*, 225–232.
31. Vallbo, A.B.; Johansson, R.S. Properties of cutaneous mechanoreceptors in the human hand related to touch sensation. *Hum Neurobiol* **1984**, *3*, 3–14.
32. Brewster, S.; Brown, L.M. Tactons: structured tactile messages for non-visual information display. In Proceedings

Preprints (www.preprints.org) | NOT PEER-REVIEWED | Posted: 28 December 2018 doi:10.20944/preprints201812.0347.v1

Peer-reviewed version available at Sensors 2019, 19, 641; doi:10.3390/s19030641

of the Proceedings of the fifth conference on Australasian user interface-Volume 28; Australian Computer Society, Inc., 2004; pp. 15–23.

33. Gunther, E.; O'Modhrain, S. Cutaneous grooves: composing for the sense of touch. *J. New Music Res.* **2003**, *32*, 369–381.
34. Sorgini, F.; Massari, L.; D'Abbraccio, J.; Palermo, E.; Menciassi, A.; Petrovic, P.B.; Mazzoni, A.; Carrozza, M.C.; Newell, F.N.; Oddo, C.M. Neuromorphic Vibrotactile Stimulation of Fingertips for Encoding Object Stiffness in Telepresence Sensory Substitution and Augmentation Applications. *Sensors* **2018**, *18*, 261.
35. Massari, L.; D'Abbraccio, J.; Baldini, L.; Sorgini, F.; Farulla, G.A.; Petrovic, P.; Palermo, E.; Oddo, C.M. Neuromorphic haptic glove and platform with gestural control for tactile sensory feedback in medical telepresence applications. In Proceedings of the 2018 IEEE International Symposium on Medical Measurements and Applications (MeMeA); IEEE, 2018; pp. 1–6.
36. Oddo, C.M.; Raspopovic, S.; Artoni, F.; Mazzoni, A.; Spigler, G.; Petrini, F.; Giambattistelli, F.; Vecchio, F.; Miraglia, F.; Zollo, L.; et al. Intraneural stimulation elicits discrimination of textural features by artificial fingertip in intact and amputee humans. *Elife* **2016**, *5*, e09148.
37. Oddo, C.M.; Mazzoni, A.; Spanne, A.; Enander, J.M.D.; Mogensen, H.; Bengtsson, F.; Camboni, D.; Micera, S.; Jörntell, H. Artificial spatiotemporal touch inputs reveal complementary decoding in neocortical neurons. *Sci. Rep.* **2017**, *7*, 45898.
38. Rongala, U.B.; Mazzoni, A.; Oddo, C.M. Neuromorphic Artificial Touch for Categorization of Naturalistic Textures. *IEEE Trans. Neural Networks Learn. Syst.* **2015**, 1–11.
39. Sorgini, F.; Mazzoni, A.; Massari, L.; Caliò, R.; Galassi, C.; Kukreja, S.L.; Sinibaldi, E.; Carrozza, M.C.; Oddo, C.M. Encapsulation of piezoelectric transducers for sensory augmentation and substitution with wearable haptic devices. *Micromachines* **2017**, *8*, 270.
40. Izhikevich, E.M. Simple model of spiking neurons. *IEEE Trans. Neural Networks* **2003**, *14*, 1569–1572.
41. Hodgkin, A.L.; Huxley, A.F. A quantitative description of membrane current and its application to conduction and excitation in nerve. *J. Physiol.* **1952**, *117*, 500–544.
42. Izhikevich, E.M. Which model to use for cortical spiking neurons? *IEEE Trans. Neural Networks* **2004**, *15*, 1063–1070.
43. Miller, J.; Ulrich, R. On the analysis of psychometric functions: The Spearman-Kärber method. *Percept. Psychophys.* **2001**, *63*, 1399–1420.
44. Samani, A.; Zubovits, J.; Plewes, D. Elastic moduli of normal and pathological human breast tissues: an inversion-technique-based investigation of 169 samples. *Phys. Med. Biol.* **2007**, *52*, 1565.
45. Zhang, M.; Nigwekar, P.; Castaneda, B.; Hoyt, K.; Joseph, J. V; di Sant'Agnese, A.; Messing, E.M.; Strang, J.G.; Rubens, D.J.; Parker, K.J. Quantitative characterization of viscoelastic properties of human prostate correlated with histology. *Ultrasound Med. Biol.* **2008**, *34*, 1033–1042.
46. Winstone, B.; Melhuish, C.; Pipe, T.; Callaway, M.; Dogramadzi, S. Toward Bio-Inspired Tactile Sensing Capsule Endoscopy for Detection of Submucosal Tumors. *IEEE Sens. J.* **2017**, *17*, 848–857.